

Rational approximation for estimation of quality Q factor and phase velocity in linear, viscoelastic, isotropic media

Dali Zhang · Michael P. Lamoureux ·
Gary F. Margrave · Elena Cherkaev

Received: 3 September 2009 / Accepted: 5 July 2010
© Springer Science+Business Media B.V. 2010

Abstract The article presents a numerical inversion method for estimation of quality Q factor and phase velocity in linear, viscoelastic, isotropic media using reconstruction of relaxation spectrum from measured or computed complex velocity or modulus of the medium. Mathematically, the problem is formulated as an inverse problem for reconstruction of relaxation spectrum in the analytic Stieltjes representation of the complex modulus using rational approximation. A rational (Padé) approximation to the relaxation spectrum is derived from a constrained least squares minimization problem with regularization. The recovered stress-strain relaxation spectrum is applied to numerical calculation of frequency-dependent Q factor and frequency-dependent phase velocity for known analytical models of a standard linear viscoelastic solid

(Zener) model as well as a nearly constant- Q model which has a continuous spectrum. Numerical results for these analytic models show good agreement between theoretical and predicted values and demonstrate the validity of the algorithm. The proposed method can be used for evaluating relaxation mechanisms in seismic wavefield simulation of viscoelastic media. The constructed lower order Padé approximation can be used for determination of the internal memory variables in time-domain finite difference numerical simulation of viscoelastic wave propagation.

Keywords Stieltjes representation · Rational approximation · Relaxation spectrum · Quality factor · Complex velocity · Viscoelastic modulus

Mathematics Subject Classification (2010) 41A20 · 86-08 · 45Q05

D. Zhang (✉) · M. P. Lamoureux
Department of Mathematics and Statistics,
University of Calgary, 2500 University Drive NW,
Calgary, Alberta, T2N 1N4, Canada
e-mail: dlzhang@math.ucalgary.ca

M. P. Lamoureux
e-mail: mikel@math.ucalgary.ca

G. F. Margrave
Department of Geoscience, University of Calgary,
2500 University Drive NW, Calgary, Alberta,
T2N 1N4, Canada
e-mail: margrave@ucalgary.ca

E. Cherkaev
Department of Mathematics, University of Utah,
155 S 1400 E, JWB 233, Salt Lake City, UT 84112-0090, USA
e-mail: elena@math.utah.edu

1 Introduction

This paper presents a novel approach to forward and inverse modeling of the quality factor Q and the relaxation spectrum using low-order Padé approximation. We consider a homogeneous isotropic one-dimensional (1D) viscoelastic medium in which the material physical properties are spatially independent. The problem is formulated as an approximation of the relaxation spectrum based on rational (Padé) approximation of the Stieltjes representation of the complex modulus. The constructed Padé approximation is used to extract relaxation parameters (spectrum) of the medium and

to estimate the phase velocity in linear, viscoelastic, isotropic media. The data are provided by frequency-dependent measured or simulated values of complex velocity or complex modulus. Using the recovered stress-strain relaxation parameters, the quality Q factor and phase velocity of wave propagating in such viscoelastic medium can then be calculated. A numerical method of construction of the Padé approximation is based on a constrained least squares minimization, regularized by the constraints derived from the analytic Stieltjes representation of the complex modulus. Solution of the constrained minimization problem gives us coefficients of the rational approximation to the relaxation spectrum of the medium. This rational approximation is transformed into Padé approximation by partial fraction decomposition. The method can use as input data the values of measured, simulated, or desired complex velocity or modulus in a certain interval of frequencies. The recovered lower order rational ($[p, q]$ -Padé) approximation can be used for determination of the internal memory variables in time-domain finite difference (TDFD) numerical simulation of viscoelastic wave propagation.

Our longterm goal is to combine this technique with finite difference (FD) modeling to give an alternative formulation for numerical simulation of viscoelastic wave propagation. The present approach also suggests a new simultaneous inversion technique for estimation of the frequency-dependent complex velocities, Q factors and phase velocities in anelastic media from vertical seismic profile (VSP) data in geophysics prospecting.

The paper is organized as follows: Section 2 gives a brief review of the relevant literature. Section 3 introduces an analytic representation of complex modulus and derives a discrete partial fraction approximation of complex modulus for inverse modeling of quality factor Q and estimation of the frequency-dependent phase velocity. We derived an error estimate of the proposed approximation method, which is given in the [Appendix](#). A new numerical algorithm of rational (Padé) approximation to the relaxation spectrum of the medium is presented in Section 4. In Section 5, we derive the analytic representations for a standard linear viscoelastic solid (Zener) model and for a viscoelastic model with continuous spectrum. These representations are used in the next section to numerically demonstrate the efficiency of the method. Numerical experiments of approximation of the relaxation spectrum for known analytic viscoelastic models and the calculated estimates of Q factors and phase velocities are shown in Section 6.

2 Literature review

The analytical Stieltjes integral representation of the complex modulus in a linear isotropic viscoelastic material was first introduced in [12] for modeling of internal memory variables in the TDFD calculations of plane-wave propagation through a constant Q medium. The complex viscoelastic modulus characterizing the attenuation and dispersion effects of a viscoelastic medium was modeled using Padé approximations in the frequency domain. The method of construction of Padé approximations was based on finding the zeros of orthogonal polynomials to determine the poles of the rational approximate for a constant relaxation spectrum (see section 3.2 of Day's paper) and deriving Padé approximation of the stress-strain relation. The viscoelastic stress-strain relation in the time domain was transformed into a differential form by introducing internal memory variable functions. This results in a system of first-order differential equations for the unknown internal variable functions to be solved together with the wave equation of motion in viscoelastic wave-field numerical simulations. The approach developed in [12] can be viewed in the time-domain as the replacement of the convolution operator by a low-order differential operator. The memory variable technique developed in [12] provides a powerful tool for the incorporation of anelasticity into numerical wave propagation methods. Such methods include FD methods [15, 24, 30], hybrid methods [17], and Fourier or Chebyshev pseudo-spectral techniques [7, 8, 23, 31] for seismic wave modelling in realistic (complex) media.

The accuracy of wave propagation through an attenuating medium simulated using the introduced internal variables, depends on how the time-dependent relaxation function of stress-strain is modeled. Rheological models such as the Generalized Maxwell Body (GMB) model and the Standard Linear Solid (SLS) model are commonly used in numerical simulations of viscoelastic wave field [5, 16, 39], they describe the stress-strain relation as a convolution of a linear combination of relaxation functions in the time domain. The behavior of each single relaxation function is controlled by constant coefficients of a weight factor and a relaxation time. The GMB and SLS models are completely specified by the number of relaxation functions associated with these constant coefficients based on the requirement that the quality factor Q , which is usually formulated as a function of temporal frequency, must be nearly constant within an assigned frequency band. However, the number of different relaxation functions is proportional to the number of the introduced internal memory

variables, this directly affects the computer storage and computation time of TDFD numerical calculations. In order to reduce the computation cost, [13, 14] proposed a coarse-grained method by using only one memory variable for each stress component of each node. The stability and analysis of the coarse-grain viscoelastic simulation was given in [21].

Attenuation and dispersion of a viscoelastic medium are often characterized by a quality factor Q . Many algorithms to estimate Q factor and phase velocity have been published. An inversion method for estimating frequency-dependent phase velocities and frequency-dependent Q factors in anelastic medium from both synthetic and real zero-offset VSP data acquired in a medium with plane horizontal layers was developed in [1]. Techniques using spectral method for estimation of quality Q factors from surface seismic common midpoint gathers (surface seismic reflection data) were presented in [11, 40]. A Gabor deconvolution algorithm to correct reflection seismograms for the effects of elastic attenuation and source signature has been developed in [27, 28]. An extensive comparison of different techniques of the frequency-dependent attenuation of seismic waves from VSP data has been investigated in [33, 35] and numerical comparison of seismic plane-wave dispersion and attenuation models has been reported in [34]. Computation techniques for stabilizing inverse Q filtering were studied in [36, 37, 41]. Efficient modeling of Q factors for 3D TDFD simulation of wave propagation was developed in [25].

3 Analytic representation of viscoelastic modulus

We consider a plane compressional wave propagating in a homogeneous isotropic dissipative medium with constant material properties. The equation of motion and the relation between stress σ and strain ε for 1D linear viscoelastic media are represented by

$$\rho \frac{\partial^2 u}{\partial t^2} = \frac{\partial \sigma}{\partial x}, \tag{1}$$

and

$$\sigma = \mathcal{M} * d\varepsilon = \int_{-\infty}^t \mathcal{M}(t - \tau) d\varepsilon(\tau), \quad \varepsilon = \frac{\partial u}{\partial x} \tag{2}$$

where ρ is the mass density, $u(\mathbf{x}, t)$ is the displacement, $\mathcal{M}(t)$ is the relaxation function or medium modulus.

In the frequency domain, the relation between stress σ and strain ε in (2) can be formulated as

$$\sigma(\omega) = M(\omega)\varepsilon(\omega) \tag{3}$$

where $M(\omega)$ is the complex viscoelastic modulus and ω is the angular frequency. The complex velocity and the phase velocity in an attenuating medium are given by (see (2.80) & (2.83), p. 61 in ref. [9])

$$V(\omega) = \sqrt{\frac{M(\omega)}{\rho}} \tag{4}$$

and

$$\frac{1}{c(\omega)} = \text{Re} \left[\left(\frac{\rho}{M(\omega)} \right)^{1/2} \right] \tag{5}$$

respectively, where ρ is the density of the medium. The dimensionless quality factor Q as a function of ω is defined as

$$Q(\omega) = \frac{\text{Re}M(\omega)}{\text{Im}M(\omega)} = \cot \theta(\omega) \tag{6}$$

where $\theta(\omega)$ is the phase of M . $M(\omega)$ is uniquely determined by a given $Q(\omega)$ in a causal medium since $\text{Re}M$ and $\text{Im}M$ must obey Kramers–Kronig dispersion relations (see (2.70) and (2.72) in [9]). The quality Q factor characterizes the phase delay between the oscillating stress and strain. In seismic applications, the quality factor Q is normally assumed to be frequency independent or only slowly varying with frequency [22]. The Q factor is commonly used for evaluating the absorption and attenuation of the seismic wave.

Recall the integral expression for the viscoelastic modulus M (see (8) in [12])

$$M(\omega) = M_U - \delta M \int_0^\infty \frac{d\eta(x)}{i\omega + x} \tag{7}$$

where $d\eta(x) = \Phi(-\ln x)dx$ and the imaginary unit $i = \sqrt{-1}$. The non-negative distribution $\Phi(\ln\tau)$ is called the normalized relaxation spectrum of the medium with $\tau = x^{-1}$ being the relaxation time. Here, M_U is the unrelaxed modulus and δM is the relaxation of the

modulus. In terms of $M(\omega)$, it is seen from (7) that M_U , the relaxed modulus M_R , and δM are given by

$$M_U = \lim_{\omega \rightarrow \infty} M(\omega), \quad M_R = \lim_{\omega \rightarrow 0} M(\omega), \quad \delta M = M_U - M_R. \tag{8}$$

This results in the following normalization of the function η :

Proposition 1 [12] *The function η has the following property (sum rule)*

$$\int_0^\infty \frac{d\eta(x)}{x} = 1. \tag{9}$$

The justification of this proposition easily follows from Eqs. 5 to 9 in [12] with the change of variable $x = \tau^{-1}$.

It is convenient to introduce a new complex variable $s = i\omega$ and define a new function $G(s) = (M_U - M(s/i))/\delta M$ which is the integral part of the complex modulus $M(\omega)$ defined in (7). The function G can be written as

$$G(s) = \frac{M_U - M(s/i)}{\delta M} = \int_0^\infty \frac{d\eta(x)}{s+x}, \quad s \in \mathbb{C} \setminus (-\infty, 0) \tag{10}$$

where η is the non-negative measure on $[0, \infty)$ which characterizes the relaxation spectrum of the medium. The function $G(s)$ is analytic outside the negative real semiaxis in the complex s -plane, all its singular points are in the interval $(-\infty, 0)$. The real-valued function $\eta(x)$ is uniquely determined if it is chosen such that

$$\eta(x) = \eta(x^+), \quad \eta(0) = 0, \tag{11}$$

and it can be obtained from the function G by the Stieltjes inversion formula [38]

$$\eta(x) = \frac{\eta(x^+) + \eta(x^-)}{2} = -\frac{1}{\pi} \lim_{y \rightarrow 0^+} \int_0^x \text{Im} G(-\nu + iy) d\nu. \tag{12}$$

Equation 10 is a Stieltjes analytic representation of the viscoelastic modulus similar to the analytic integral representation of the effective complex permittivity which was developed for computing bounds for the effective permittivity of an arbitrary two-phase composite [3, 4, 19, 29]. The uniqueness of reconstruction

of the spectral measure in the analytic Stieltjes representation of the effective complex permittivity was discussed in [10] where it was shown that the spectral measure can be uniquely recovered if measurements of the effective property are available on an arc in a complex plane. Because the complex velocity $V(\omega)$ in (4) or complex viscoelastic modulus $M(\omega)$ in (7) is frequency dependent, the measurements of $V(\omega)$ or $M(\omega)$ at certain frequencies should be able to provide the desired data set.

Based on the theory of reconstruction of the spectral measure developed in [10] and the approach to reconstruction of the spectral measure of effective permittivity of a composite material using rational function approximations in [42, 43], the function $\eta(x)$ can be approximated by a step function with a finite number of steps, so that

$$d\eta(x) \simeq d\hat{\eta}(x) = \sum_{n=1}^q A_n \delta(x + \rho_n) dx. \tag{13}$$

For $A_n > 0$ and $\rho_n < 0$ where $-\infty < \rho_q < \dots < \rho_2 < \rho_1 < 0$, the function $\eta(x)$ satisfying (11) can be approximated by

$$\begin{aligned} \eta(x) &= \int_0^{x^+} d\eta(t) \simeq \int_0^{x^+} d\hat{\eta}(t) \\ &= \int_0^{x^+} \sum_{n=1}^q A_n \delta(t + \rho_n) dt \\ &= \sum_{n=1}^q A_n \int_0^{x^+} \delta(t + \rho_n) dt \end{aligned} \tag{14}$$

so that

$$\eta(x) \simeq \hat{\eta}(x) = \sum_{n=1}^q A_n H(x + \rho_n), \tag{15}$$

where $H(x)$ is the Heaviside step function. The function $\eta(x)$ defined for $x \in [0, \infty)$ is a non-decreasing, non-negative function corresponding to the Stieltjes function $G(s)$. Thus, the approximation $\hat{G}(s)$ of the function $G(s)$ is given by

$$G(s) \simeq \hat{G}(s) = \sum_{n=1}^q \frac{A_n}{s - \rho_n}, \tag{16}$$

with constraints

$$-\infty < \rho_n < 0, \quad 0 < \frac{A_n}{|\rho_n|} < 1, \quad \sum \frac{A_n}{|\rho_n|} = 1. \tag{17}$$

Here ρ_n is the n -th simple pole on the negative real semiaxis with positive residue A_n , q is the total number of poles. It follows from (10), (13), and (16) that

the approximation of the complex modulus $M(\omega)$ is given by

$$M(\omega) \simeq M_U - \delta M \sum_{n=1}^q \frac{A_n}{i\omega - \rho_n}. \tag{18}$$

Equation 18 gives an expression of discrete approximation of the complex modulus $M(\omega)$ in a partial fraction form. The real parameters A_n and ρ_n in this representation contain all information about the relaxation spectrum of the medium. It follows from (6) and (18), that the quality Q factor, the complex velocity $V(\omega)$ and the phase velocity $c(\omega)$ can be estimated in terms of A_n and ρ_n as

$$Q(\omega) \simeq \frac{\text{Re} \left[M_U - \delta M \sum_{n=1}^q \frac{A_n}{i\omega - \rho_n} \right]}{\text{Im} \left[M_U - \delta M \sum_{n=1}^q \frac{A_n}{i\omega - \rho_n} \right]}, \tag{19}$$

$$V(\omega) \simeq V^c(\omega) = \frac{1}{\sqrt{Q}} \left\{ M_U - \delta M \sum_{n=1}^q \frac{A_n}{i\omega - \rho_n} \right\}^{\frac{1}{2}} \tag{20}$$

and

$$c(\omega) \simeq \frac{1}{\text{Re} V^c(\omega)}, \tag{21}$$

respectively.

The partial fraction approximation (18) for the complex modulus $M(\omega)$ implies the relationship between the stress σ and strain ε in the time domain as shown in [12] as

$$\sigma(t) = M_U \left[\varepsilon(t) - \sum_{n=1}^q \zeta_n(t) \right] \tag{22}$$

where ζ_n ($n = 1, 2, \dots, q$) are the internal memory variables which satisfy the first-order differential equations [12, 16, 24]

$$\frac{d\zeta_n(t)}{dt} - \rho_n \zeta_n(t) = A_n \frac{\delta M}{M_U} \varepsilon(t), \quad (n = 1, 2, \dots, q). \tag{23}$$

Equation 22 represents the stress σ as a sum of the elastic part $M_U \varepsilon(t)$ and an anelastic part given by the internal memory variable functions $\zeta_n(t)$ ($n = 1, 2, \dots, q$).

Substituting Eqs. 22–23 into Eqs. 1–2 results in the system of governing differential equations [16, 24, 44]

$$\varrho \frac{\partial^2 u}{\partial t^2} = M_U \left[\frac{\partial^2 u}{\partial \mathbf{x}^2} - \sum_{n=1}^q \vartheta_n(\mathbf{x}, t) \right] \tag{24}$$

where $\vartheta_n(\mathbf{x}, t) = \frac{\partial \zeta_n}{\partial \mathbf{x}}(\mathbf{x}, t)$ satisfies

$$\frac{d\vartheta_n}{dt} - \rho_n \vartheta_n = A_n \frac{\delta M}{M_U} \frac{\partial^2 u}{\partial \mathbf{x}^2}, \quad (n = 1, 2, \dots, q). \tag{25}$$

Comparing to 1D viscoelastic Eqs. 1–2, the convolution integral is eliminated in the system of Eqs. 24–25 by introducing a sequence of variables ϑ_n . The internal function ϑ_n satisfies a first-order differential Eq. 25 in time. Equations 25 have to be solved for the unknown functions ϑ_n in addition to the wave Eq. 24 of motion in the time-domain numerical simulation of wave propagations using FD methods. The accuracy of numerical computation of wave propagation in an attenuating medium depends on how well the poles ρ_n and residues A_n of the function $G(s)$ are determined when using Eqs. 22–25. From a practical computation point of view, it is important (crucial) to keep the number of internal memory variable functions ζ_n in (23) or ϑ_n in (25) as low as possible. This yields to construct a lower order rational approximation of complex modulus $M(\omega)$ for modeling of quality factor Q in the frequency domain.

Let us assume that the complex velocity $V(\omega)$ or complex modulus $M(\omega)$ can be measured or computed in a range of frequencies or can be modeled for a specific viscoelastic material. We describe an inversion method in Section 4 which allows us to identify the real parameters A_n and ρ_n , and to construct a rational ($[p, q]$ -Padé) approximation of $M(\omega)$ in (18), especially for a lower order $[p, q]$ -Padé approximation of $M(\omega)$ from measured or computed complex velocity. Therefore, the quality factor Q and phase velocity $c(\omega)$ can be evaluated using formula (19) and (21), respectively.

Remark 1 For a homogeneous medium, the unrelaxed modulus M_U and the relaxed modulus M_R in (8) are constants. Equations 24–25 with appropriate initial and boundary conditions can be solved numerically using FD method. For more complex and heterogenous media, the relaxation function $\mathcal{M}(t)$ in (2), the complex modulus $M(\omega)$ in (7), as well as the mass density function ϱ and the unrelaxed modulus M_U in (24) are spatially dependent. To extend our approach to a heterogeneous medium, the real parameters δM , A_n , and ρ_n in (25) should be placed an emphasis on spatial

dependence. Generalization to the 2D FD simulation of viscoelastic shear wave propagation was done in [16].

Remark 2 In Appendix, we present the detailed proofs of an error estimate of the proposed approximation method described in Eqs. 13–17.

4 Rational approximation for inversion

In this section, we present a new numerical inversion method for approximation of the function $d\eta$ as described in Section 3 from known measured data. The approach is based on the theory of inverse homogenization [10] and the rational approximation of the spectral measure introduced in [42, 43]. We solve the inverse problem by constructing a constrained partial fraction decomposition of rational (Padé) approximation to the relaxation spectrum calculated using numerically simulated values of measurements of complex velocity. The constraints for the poles and residues of the partial fractions are given in (17) for the function $G(s)$. The Padé approximation of the function $G(s)$ is obtained by solving for the coefficients in a least squared sense after expressing the constraints as linear equations in these coefficients.

4.1 Rational ($[p, q]$ -Padé) approximation for $G(s)$

We note that the function $G(s)$ has a discrete approximation $\hat{G}(s)$ of the partial fraction form (16) as described in Section 3. Therefore, the right hand side of (16) can be approximated by an appropriate rational function

$$\hat{G}(s) = \sum_n \frac{A_n}{s - \rho_n} \simeq \frac{\phi(s)}{\psi(s)} \tag{26}$$

where ρ_n is the n -th simple pole on the negative real axis with positive real residue A_n , and the degree of the polynomial $\phi(s)$ is lower than the degree of the polynomial $\psi(s)$. Let p and q be the orders of polynomials $\phi(s)$ and $\psi(s)$ with $p < q$, respectively. The rational ($[p, q]$ -Padé) approximation of $G(s)$ can be written as (see [2, 6])

$$\hat{G}(s) = \frac{\phi(s)}{\psi(s)} = \frac{a_0 + a_1s + a_2s^2 + \dots + a_p s^p}{b_0 + b_1s + b_2s^2 + \dots + b_q s^q} \tag{27}$$

where a_l ($l = 0, 1, \dots, p$) and b_k ($k = 0, 1, \dots, q$) are the coefficients of the real polynomials $\phi(s)$ and $\psi(s)$, respectively.

Let us suppose that the function $G(s)$ has at least one pole, and all the poles of the denominator $\psi(s)$ are

simple. This assumption can be viewed as an approximation of the function $d\eta$ by a sum of the finite number of Dirac measure in (13). Since the poles ρ_n of the function $G(s)$ lie in the interval $(-\infty, 0)$, we normalize the polynomial coefficient $b_0 = 1$ in the denominator $\psi(s)$ which allows us to identify the non-zero poles of G . To derive the linear system of equations for the coefficients a_l 's and b_k 's in (27), we further assume that the measured data pairs (s_j, g_j) ($j = 1, 2, \dots, N$) of the function G are given by: $g_j = G(s_j)$, $s_j = i\omega_j$, and the imaginary unit $i = \sqrt{-1}$. Here ω_j is the frequency sample data point and N is the total number of the complex measured values of $G(s)$. We require that the constructed approximation $\hat{G}(s)$ agrees with the measured values of $G(s)$ at the points s_j . Then Eq. 27 can be written as

$$\frac{\phi(s_j)}{\psi(s_j)} = \frac{a_0 + a_1s_j + a_2s_j^2 + \dots + a_p s_j^p}{1 + b_1s_j + b_2s_j^2 + \dots + b_q s_j^q} = g_j \tag{28}$$

where a_l ($l = 0, \dots, p$), b_k ($k = 1, \dots, q$) are required unknown coefficients. Equation 28 is equivalent to the following system

$$a_0 + a_1s_j + \dots + a_p s_j^p - b_1g_j s_j - b_2g_j s_j^2 - \dots - b_q g_j s_j^q = g_j \tag{29}$$

for $j = 1, 2, \dots, N$. Therefore, the system (29) for the unknown coefficients a_l 's and b_k 's of the ratio $\phi(s)/\psi(s)$ in (27) can be further expressed as the following system

$$\mathbf{S}\mathbf{c} := \mathbf{g} \tag{30}$$

where

$$\mathbf{S} = \begin{pmatrix} 1 & s_1 & \dots & s_1^p & -g_1s_1 & -g_1s_1^2 & \dots & -g_1s_1^q \\ 1 & s_2 & \dots & s_2^p & -g_2s_2 & -g_2s_2^2 & \dots & -g_2s_2^q \\ \dots & \dots \\ 1 & s_N & \dots & s_N^p & -g_Ns_N & -g_Ns_N^2 & \dots & -g_Ns_N^q \end{pmatrix}$$

$$\mathbf{c} = [a_0, a_1, \dots, a_p, b_1, \dots, b_q]^\top, \mathbf{g} = [g_1, g_2, \dots, g_N]^\top, \tag{31}$$

the symbol $[\cdot]^\top$ indicates a transposed matrix. It is clear that in order for the Padé coefficients a_l 's and b_k 's to be uniquely determined, the total number of the measurements is required to be greater or equal to the number of coefficients, i.e., $N \geq p + q + 1$. The reconstruction problem of determining the column real coefficient vector $\mathbf{c} = [a_0, a_1, \dots, a_p, b_1, b_2, \dots, b_q]^\top$ in (30) is an inverse problem. It is ill-posed and requires regularization to develop a stable numerical algorithm.

In the present work, we solve a constrained minimization problem described below with constraints given in (17).

4.2 Inversion method

Let define complex matrices $\mathbf{S} = \mathbf{S}_R + i\mathbf{S}_I$ and $\mathbf{g} = \mathbf{g}_R + i\mathbf{g}_I$, where subindices R and I indicate the real and imaginary parts of the matrices with entries in terms of data, and the imaginary unit $i = \sqrt{-1}$. To construct a real solution vector \mathbf{c} of $[p, q]$ -Padé coefficients for the inverse problem (30), we formulate the least squares problem as

$$\min_{\mathbf{c}} \{ \|\mathbf{S}\mathbf{c} - \mathbf{g}\|^2 \} \iff \min_{\mathbf{c}} \{ \|\mathbf{S}_R\mathbf{c} - \mathbf{g}_R\|^2 + \|\mathbf{S}_I\mathbf{c} - \mathbf{g}_I\|^2 \}. \tag{32}$$

Here $\|\cdot\|$ is the usual Euclidean norm. The solution of the minimization problem (32) usually does not continuously depend on the data, the problem requires a regularization technique. As a widely used approach for solving ill-posed problems, the Tikhonov regularization was applied to (32) with introducing a penalization term in the Tikhonov regularization functional $\mathcal{T}^\lambda(\mathbf{c}, \mathbf{g}_R, \mathbf{g}_I)$, so that the problem (32) can be reformulated as the following unconstrained minimization problem [32]

$$\min_{\mathbf{c}} \mathcal{T}^\lambda(\mathbf{c}, \mathbf{g}_R, \mathbf{g}_I) = \min_{\mathbf{c}} \{ \|\mathbf{S}_R\mathbf{c} - \mathbf{g}_R\|^2 + \|\mathbf{S}_I\mathbf{c} - \mathbf{g}_I\|^2 + \lambda^2\|\mathbf{c}\|^2 \} \tag{33}$$

Here $\lambda > 0$ is a regularization parameter to be chosen properly. However, the problem (33) is still ill-posed due to the noise present in the elements of the matrices \mathbf{S}_R and \mathbf{S}_I as well as in the right-hand side vector \mathbf{g} , so that both the coefficient matrices and the right-hand side vector are not precisely known. The total least squares method could be used for solving this kind of linear least squares problems [18, 20]. Application of this method will not be considered in this paper. In the present approach, inequalities in (17) for the residues and poles of the function $G(s)$ are used explicitly in the algorithm to impose constraints for the set of minimizers of the problem. Therefore, the regularized Tikhonov solution \mathbf{c} for the problem (30) is obtained

as a solution of the following constrained least squares minimization problem [42, 43]

$$\min_{\mathbf{c}} \mathcal{T}^\lambda(\mathbf{c}, \mathbf{g}_R, \mathbf{g}_I) = \min_{\mathbf{c}} \{ \|\mathbf{S}_R\mathbf{c} - \mathbf{g}_R\|^2 + \|\mathbf{S}_I\mathbf{c} - \mathbf{g}_I\|^2 + \lambda^2\|\mathbf{c}\|^2 \} \tag{34}$$

s.t. $-\infty < \rho_n < 0, 0 < \frac{A_n}{|\rho_n|} < 1, n = 1, 2, \dots, q.$

Here parameters A_n and ρ_n in the constraints (34) are residues and poles of the partial fractions decomposition of the reconstructed $[p, q]$ -Padé approximation of the function $G(s)$. The corresponding Euler equation of the problem (34) is given by

$$\mathbf{c} = \{ \mathbf{S}_R^T \mathbf{S}_R + \mathbf{S}_I^T \mathbf{S}_I + \lambda \mathbf{I}_{p+q+1} \}^{-1} \{ \mathbf{S}_R^T \mathbf{g}_R + \mathbf{S}_I^T \mathbf{g}_I \} \tag{35}$$

where \mathbf{I}_{p+q+1} denotes the $(p + q + 1) \times (p + q + 1)$ identity matrix.

After reconstruction of the real coefficient vector \mathbf{c} of the rational function approximation $\hat{G}(s)$, its decomposition into partial fractions (26) will give $[p, q]$ -Padé approximation of $G(s)$. The reconstructed function $\hat{G}(s)$ can be used to identify the relaxation spectrum for a viscoelastic medium and to estimate the quality Q factor for such a medium using formula (19).

5 Analytic representation for standard models

The aim of this section is to derive an analytic representation for standard viscoelastic models. We consider a standard linear viscoelastic solid model with a discrete spectrum as well as a nearly constant- Q model with a continuous spectrum. These analytic models are used in numerical simulations to examine the effectiveness of the inversion method developed in Section 4.

5.1 Standard linear viscoelastic solid model

We consider the time-dependent relaxation function of stress-strain relation in a standard linear solid (Generalized Zener) model [7, 8]

$$\mathcal{M}(t) = M_R \left[1 - \sum_{n=1}^L \left(1 - \frac{\tau_{\epsilon_n}}{\tau_{\sigma_n}} \right) e^{-t/\tau_{\sigma_n}} \right] H(t) \tag{36}$$

where $\tau_{\epsilon_n} \geq \tau_{\sigma_n}, \tau_{\epsilon_n}, \tau_{\sigma_n}$ denote material strain relaxation time and stress relaxation time for the n -th mechanism, respectively. This model was also introduced

Table 1 True values of relaxation times for five mechanisms to yield a constant $Q = 100$ ($\omega = 2 \sim 50$ Hz) for the synthetic viscoelastic modulus given in [31]

n	1	2	3	4	5
τ_{ϵ_n} (s)	0.3196389	0.0850242	0.0226019	0.0060121	0.0016009
τ_{σ_n} (s)	0.3169863	0.0842641	0.0224143	0.0059584	0.0015823

in [5, 26, 31, 39] in order to obtain a nearly constant quality Q factor over the seismic frequency range of interest. Here the relaxed modulus $M_R = M_U - \delta M$, L is the number of relaxation mechanisms, and $H(t)$ is the heaviside step function. The unrelaxed modulus

$$M_U = M_R \left[1 - \sum_{n=1}^L \left(1 - \frac{\tau_{\epsilon_n}}{\tau_{\sigma_n}} \right) \right] \tag{37}$$

is obtained for $t = 0$ in (36). Applying the Laplace transform in s -multiplied form (see (7) in [12]), i.e.,

$$F(s) = s \int_0^\infty \mathcal{F}(t)e^{-st} dt \tag{38}$$

to the stress-strain relation (36), and setting $s = i\omega$, the complex modulus can be derived as

$$M(\omega) = M_R \left[1 - \sum_{n=1}^L \left(1 - \frac{\tau_{\epsilon_n}}{\tau_{\sigma_n}} \right) \frac{i\omega}{i\omega + \tau_{\sigma_n}^{-1}} \right]. \tag{39}$$

Noticing (37) and the definition of function $G(s)$ in (10), corresponding to the complex modulus $M(\omega)$ (39), $G(s)$ is found in the following L -term partial fractions form

$$G(s) = \left(\frac{M_U}{M_R} - 1 \right)^{-1} \sum_{n=1}^L \frac{(\tau_{\epsilon_n}/\tau_{\sigma_n} - 1)\tau_{\sigma_n}^{-1}}{s + \tau_{\sigma_n}^{-1}}. \tag{40}$$

In the complex s -plane, Eq. 40 implies a representation for the poles and residues of the function $G(s)$:

$$\rho_n = -\tau_{\sigma_n}^{-1}, \tag{41}$$

$$A_n = (M_U/M_R - 1)^{-1} [(\tau_{\epsilon_n}/\tau_{\sigma_n} - 1) \tau_{\sigma_n}^{-1}] \tag{42}$$

where $1 \leq n \leq L$. The location of poles and residues of the function G depends on the strain-stress relaxation

parameters τ_{ϵ_n} and τ_{σ_n} . From Eq. 37, one can check that the residues A_n and poles ρ_n in (41–42) satisfy the sum rule property as in the last equation of (17).

Let us assume that the complex velocity $V(\omega)$ or the complex modulus $M(\omega)$ can be simulated in a range of frequencies for the SLS model (39) and the real parameters A_n and ρ_n can be recovered using the reconstruction algorithm of a $[p, q]$ -Padé approximation of the function $G(s)$ as described in the previous sections. From Eqs. 41–42, we can calculate the strain-stress relaxation parameters τ_{ϵ_n} and τ_{σ_n} in terms of the recovered poles ρ_n and residues A_n of $G(s)$ explicitly as follows:

$$\tau_{\epsilon_n}^c = (M_U/M_R - 1)A_n\rho_n^{-2} - \rho_n^{-1}, \tag{43}$$

$$\tau_{\sigma_n}^c = -\rho_n^{-1} \tag{44}$$

where $1 \leq n \leq q$, the superscript c indicates the computed value of τ_{ϵ_n} and τ_{σ_n} . From formulas (41–42) and (43–44), we can see that the parameters τ_{ϵ_n} and τ_{σ_n} can be simply calculated once the poles ρ_n and residues A_n of the approximation $d\hat{\eta}(x)$ of the function $d\eta(x)$ are determined. For the SLS model (39), by the definition (6) and Eq. 39, the quality Q factor as a function of frequency ω can be estimated for different lower orders $q \leq L$ using the derived formula

$$Q^c(\omega) = \frac{1 + \sum_{n=1}^q \frac{(\tau_{\epsilon_n}^c - \tau_{\sigma_n}^c)\omega^2\tau_{\sigma_n}^c}{1 + \omega^2(\tau_{\sigma_n}^c)^2}}{\sum_{n=1}^q \frac{(\tau_{\epsilon_n}^c - \tau_{\sigma_n}^c)\omega}{1 + \omega^2(\tau_{\sigma_n}^c)^2}} \tag{45}$$

Table 2 Reconstruction of poles and normalized residues of the function $G(s)$ corresponding to the synthetic modulus $M(s)$

n	1	2	3	4	5	$\sum A_n/ \rho_n $	q
$A_n/ \rho_n $	0.252656	0.193709	0.179893	0.193881	0.179861	1.0000000	7
ρ_n	-631.99141	-167.83029	-44.61438	-11.86745	-3.1547105		
$A_n/ \rho_n $	0.253182	0.196344	0.206661	0.317445		0.9736328	4
ρ_n	-631.21638	-166.26238	-40.83089	-6.72937			
$A_n/ \rho_n $	0.271451	0.231768	0.382293			0.8855121	3
ρ_n	-600.65191	-133.44157	-17.04249				

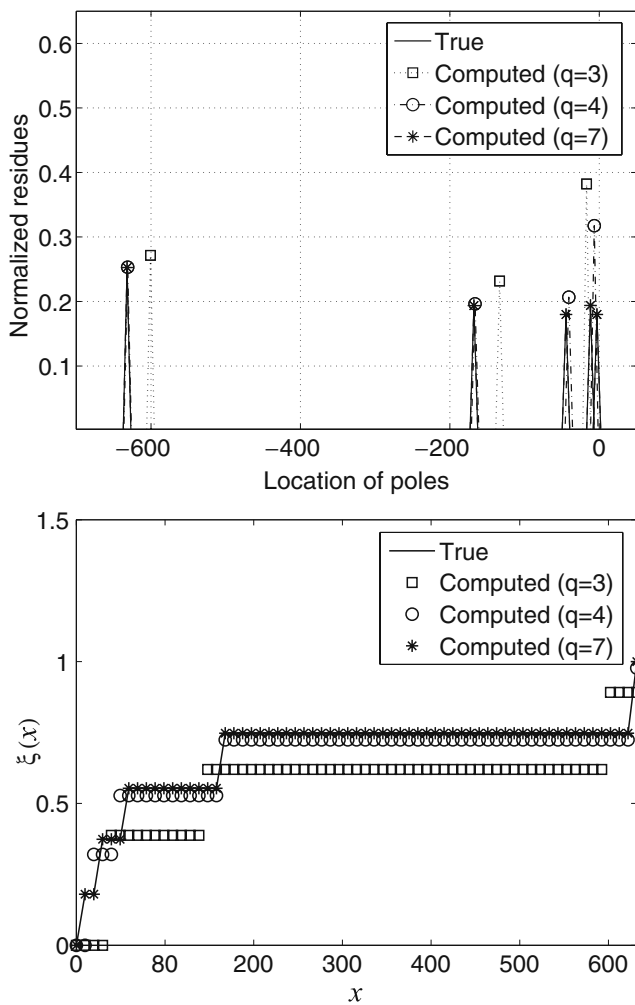


Fig. 1 Reconstruction of the normalized residues and poles of the function $G(s)$ (top) and the function $\xi(x)$ (bottom) (SLS model)

or equivalently, it can be evaluated using

$$Q^c(\omega) = \frac{M_R - \delta M \sum_{n=1}^q \frac{A_n \rho_n^{-1} \omega^2}{\omega^2 + \rho_n^2}}{\delta M \sum_{n=1}^q \frac{A_n \omega}{\omega^2 + \rho_n^2}} \quad (46)$$

where $Q^c(\omega)$ represents the calculated quality factor Q . The complex velocity can be calculated as

$$V(\omega) \simeq V^c(\omega) = \sqrt{\frac{M^c(\omega)}{\rho}} \quad (47)$$

where

$$M^c(\omega) = M_R \left[1 - \sum_{n=1}^q \left(1 - \frac{\tau_{\epsilon_n}^c}{\tau_{\sigma_n}^c} \right) \frac{i\omega}{i\omega + (\tau_{\sigma_n}^c)^{-1}} \right] \quad (48)$$

is the computed complex modulus. Therefore, the phase velocity can be calculated using (21). Furthermore, in terms of the recovered strain-stress relaxation parameters $\tau_{\epsilon_n}^c$ and $\tau_{\sigma_n}^c$, the approximation of the time-dependent relaxation function of stress-strain relation for the SLS model (36) can be represented as

$$M^c(t) = M_R \left[1 - \sum_{n=1}^q \left(1 - \frac{\tau_{\epsilon_n}^c}{\tau_{\sigma_n}^c} \right) e^{-t/\tau_{\sigma_n}^c} \right] H(t) \quad (49)$$

where $M^c(t)$ is the calculated relaxation function.

5.2 A nearly constant- Q model

We consider a nearly constant- Q model with a continuous relaxation spectrum. The synthetic function $d\eta/dx$ for this model has a constant relaxation spectrum in the finite interval $[x_0, x_1] \subset (0, \infty)$ ($x_0 \neq x_1$) given by

$$\frac{d\eta(x)}{dx} = \begin{cases} \left[\ln \left(\frac{x_1}{x_0} \right) \right]^{-1}, & \text{if } x_0 \leq x \leq x_1 \\ 0, & \text{if } x < x_0 \text{ or } x > x_1. \end{cases} \quad (50)$$

The representation of the normalized relaxation spectrum function in (56) is derived such that

$$\xi(x) = \int_0^{x^+} \frac{d\eta(t)}{t} = \begin{cases} 0, & \text{if } 0 \leq x < x_0 \\ \left[\ln \left(\frac{x_1}{x_0} \right) \right]^{-1} \ln \left(\frac{x}{x_0} \right), & \text{if } x_0 \leq x \leq x_1 \\ 1, & \text{if } x > x_1. \end{cases} \quad (51)$$

Table 3 Recovery of relaxation times for three and four mechanisms to yield a constant $Q = 100$ ($\omega = 2 \sim 50$ Hz) using the constrained Padé approximant method ($\tau_{\epsilon_n}^c, \tau_{\sigma_n}^c$ stand for the predicted values of relaxation times)

n	1	2	3	4	q
$\tau_{\epsilon_n}^c$ (s)	0.1508046	0.0247268	0.0060695	0.0016029	4
$\tau_{\sigma_n}^c$ (s)	0.1486096	0.0244912	0.0060145	0.0015842	
$\tau_{\epsilon_n}^c$ (s)	0.0597205	0.0075747	0.0016859		3
$\tau_{\sigma_n}^c$ (s)	0.0586769	0.0074939	0.0016649		

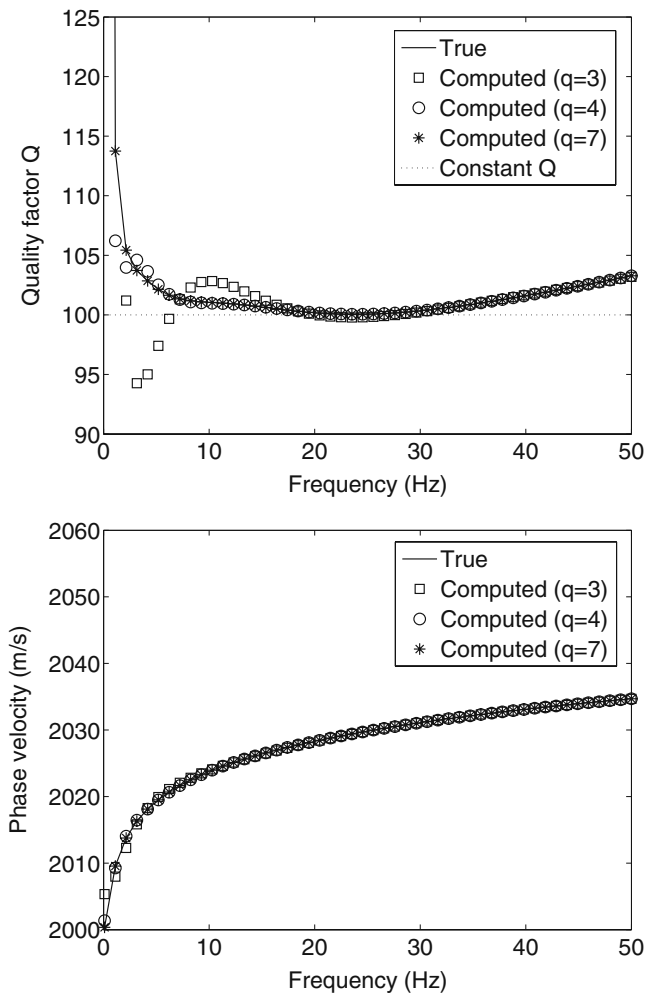


Fig. 2 True and computed quality Q factor (top) and phase velocity $c(\omega)$ (bottom) for the SLS model

It is easy to check the function $d\xi(x) = d\eta(x)/x$ in (51) satisfies the sum rule property of Proposition 1. The corresponding function G defined in (10) can be derived analytically as

$$G(s) = \int_0^\infty \frac{d\eta(x)}{s+x} = \left[\ln\left(\frac{x_1}{x_0}\right) \right]^{-1} \ln\left(\frac{s+x_1}{s+x_0}\right) \quad (52)$$

where $s = i\omega$. The corresponding complex modulus and complex velocity are obtained as

$$M(\omega) = M_U - \delta M \left[\ln\left(\frac{x_1}{x_0}\right) \right]^{-1} \ln\left(\frac{i\omega+x_1}{i\omega+x_0}\right), \quad (53)$$

and

$$V(\omega) = \left[\frac{1}{\rho} \left(M_U - \delta M \left[\ln\left(\frac{x_1}{x_0}\right) \right]^{-1} \ln\left(\frac{i\omega+x_1}{i\omega+x_0}\right) \right) \right]^{\frac{1}{2}} \quad (54)$$

respectively, where ρ is the density. The unrelaxed modulus is $M_U = \rho c_U^2$, c_U is the unrelaxed velocity, $\delta M = M_U - M_R$ is the relaxation modulus, $M_R = \rho c_R^2$, c_R is the relaxed velocity.

6 Numerical examples

In this section we present numerical experiments for reconstruction of the function $G(s)$ from frequency-dependent measurements of the complex velocity or the viscoelastic modulus using constrained rational ($[p, q]$ -Padé) approximation technique as described in Section 4 to illustrate the effectiveness of the developed inversion method. The recovered poles and residues of the function $G(s)$ are used to calculate relaxation parameters and to estimate the frequency-dependent quality Q factor and frequency-dependent phase

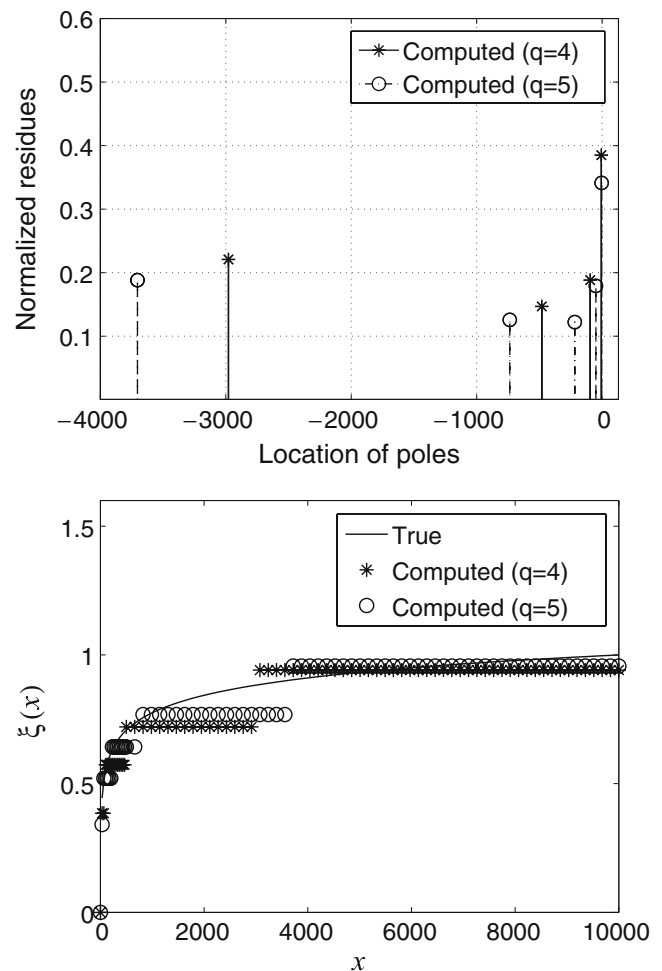


Fig. 3 Reconstruction of poles and the normalized residues of the function $G(s)$ (top) and the function $\xi(x)$ (bottom) for the continuous relaxation spectrum model

Table 4 Reconstruction of poles and normalized residues of the synthetic function $G(s)$ for the continuous spectrum model

n	1	2	3	4	5	$\sum A_n/ \rho_n $	q
$A_n/ \rho_n $	0.2208295	0.1469902	0.1883802	0.3851157		0.9413156	4
ρ_n	-2,978.2463	-480.96323	-94.802749	-5.7450234			4
$A_n/ \rho_n $	0.1882749	0.1256995	0.1223043	0.1793468	0.3413333	0.9569588	5
ρ_n	-3,704.1072	-735.70125	-217.64319	-49.240967	-3.6973038		5

velocity for a viscoelastic model with a continuous relaxation spectrum as well as for the SLS viscoelastic model (36).

6.1 Results for the SLS model

In the following numerical simulations we employ the values of material strain relaxation time τ_{ϵ_n} and stress relaxation time τ_{σ_n} shown in Table 1. The unit of the time parameters τ_{ϵ_n} and τ_{σ_n} in first column of Table 1 is in second(s). The values of these parameters τ_{ϵ_n} and τ_{σ_n} were used in Ref. [31] for numerically solving the 1-D viscoelastic equation of motion with $L = 5$ relaxation mechanisms to yield a constant quality factor $Q = 100$. Here we used these values of τ_{ϵ_n} and τ_{σ_n} to calculate the synthetic complex viscoelastic modulus $M(\omega)$ at 50 data points in the seismic exploration band of frequencies from 2 to 50 Hz.

Table 2 shows results of reconstruction of poles ρ_n and normalized residues $A_n/|\rho_n|$ of the function $G(s)$ for different orders of $q = p + 1$ chosen in the inversion algorithm when there is no noise in the data. The first row in Table 2 shows the recovered five poles and residues of the function $d\eta$ corresponding to the synthetic modulus $M(\omega)$ when $q = 7$, they are reconstructed very accurately with the computed sum $\sum A_n/|\rho_n| \approx 1.0000000$. The second and third rows present the poles and residues reconstructed with the calculated sum $\sum A_n/|\rho_n| \approx 0.9736328$ for $q = 4$ and $\sum A_n/|\rho_n| \approx 0.8855121$ for $q = 3$, respectively. The analytically and numerically calculated functions $d\xi(x)/dx$, $d\hat{\xi}(x)/dx$, $\xi(x)$, and $\hat{\xi}(x)$ are shown in Fig. 1. The top part of Fig. 1 illustrates the reconstruction of poles ρ_n and normalized residues $A_n/|\rho_n|$ for the functions $d\xi(x)/dx$ and $d\hat{\xi}(x)/dx$ using $[p, q]$ -Padé approximation with orders (1) $q = p + 1 = 3$, (2) $q = p + 1 = 4$, and (3) $q = p + 1 = 7$. The location of the recovered poles of the function G is on the negative real semiaxis. The bottom part of Fig. 1 represents the true and computed functions $\xi(x)$ and $\hat{\xi}(x)$ using formulas (56) and (57).

The recovered poles and residues of G are further used to convert the values of material strain relaxation time τ_{ϵ_n} and stress relaxation time τ_{σ_n} using formulas (43–44) with the number of relaxation mechanisms be-

ing less than 5. These reconstructed values of τ_{ϵ_n} and τ_{σ_n} are shown in Table 3 when there is no noise in the data using the lower order $q < 5$ in $[p, q]$ -Padé approximant method. In Table 3, $\tau_{\epsilon_n}^c$ and $\tau_{\sigma_n}^c$ stand for the predicted relaxation times for $L = q = 3$ and $L = q = 4$ mechanisms to yield a constant $Q = 100$ ($\omega \in 2\pi[2, 50]$ Hz) using the constrained Padé approximant method.

To estimate the frequency-dependent quality Q factor and the frequency-dependent phase velocity for the SLS model, we chose the density $\rho = 2000\text{kg/m}^3$ and the relaxed modulus $M_R = 8\text{Gpa}$ in the numerical

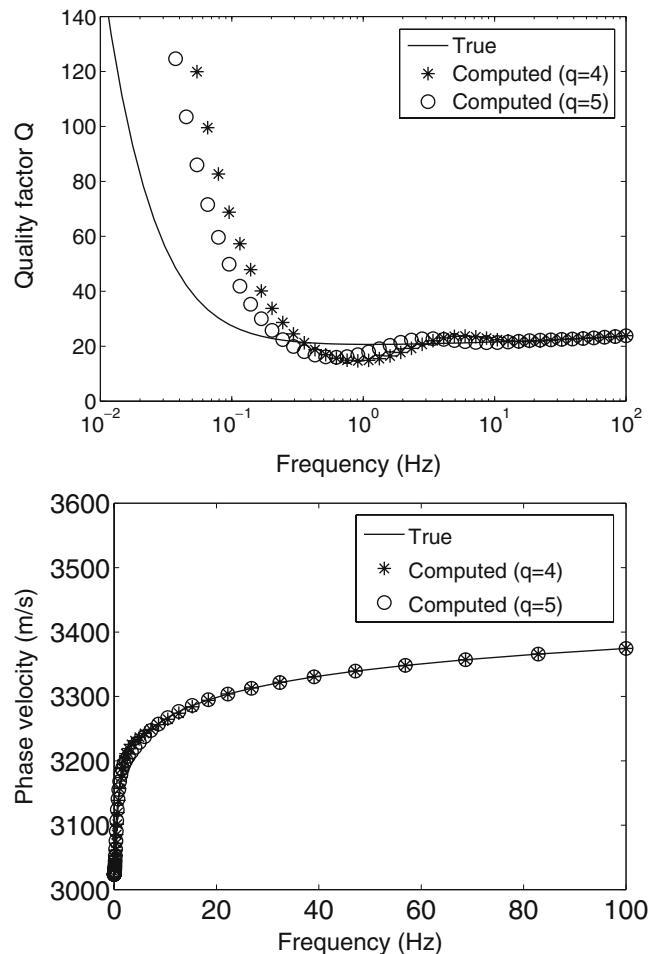


Fig. 4 Calculation of quality Q factors (top) and phase velocities $c(\omega)$ (bottom) for the continuous relaxation spectrum model using different orders of Padé approximation

Table 5 Calculated relative errors of true and computed physical parameters using formula (55)

Relative error	Phase velocity	Quality factor	Complex velocity	Complex modulus	q
E_0	1.2344214e-02	4.7875054e-01	1.2348505e-02	2.4544535e-02	4
E_0	9.1698749e-03	2.3327527e-02	9.1676003e-03	1.8251178e-02	5

simulations. Figure 2 shows the results of the recovered quality Q factors (top) and phase velocity $c(\omega)$ (bottom). It is seen from the top part of Fig. 2 that the estimated values of the quality Q factors are nearly constant $Q = 100$ over the frequency band between 12 and 37 Hz for the lower order $[p, q]$ -Padé approximant method. However, the calculated Q factors were not very good approximation to the constant $Q = 100$ in both low frequency range about $2 \sim 12$ Hz and high frequency range between 37 and 50 Hz for this particular used analytic SLS model. The estimated Q factors shown in the top Fig. 2 are calculated using equivalent formulas (45) and (46). The true and computed phase velocity versus frequency shown in the bottom Fig. 2 were calculated using formula (21). The results of computations for Q factors and phase velocity agree with the true values in published simulations of [31], especially for values at high frequencies. The calculated values of relaxation mechanisms can be used for seismic wavefield simulation in viscoelastic media.

6.2 Results for the nearly constant- Q model

In the numerical experiments for the nearly constant- Q model with a continuous relaxation spectrum (50) or (51), we chose $\rho = 2,400\text{kg/m}^3$, $c_U = 3,500\text{m/s}$, $c_R = 3,000\text{m/s}$, leading to $\delta M = 7.8\text{Gpa}$. The complex velocity measurements were simulated at 50 data points in a range of frequency as $\omega \in 2\pi[10^{-2}, 10^2]\text{s}^{-1}$, and the interval $[x_0, x_1] = [0.35, 10^4]$ was chosen for the support of the function $d\xi(x)$. The recovered normalized residues and poles of the function $G(s)$ for the continuous relaxation spectrum model are shown in the top part of Fig. 3 using the Padé approximants of different orders (1) $p + 1 = q = 4$ and (2) $p + 1 = q = 5$ when there is no noise in the data. The recovered

poles are located in the negative real semiaxis. We compared analytically and numerically calculated normalized relaxation spectrum functions. The bottom part of Fig. 3 shows the true synthetic function $\xi(x)$ and the approximation $\hat{\xi}(x)$ of the function $\xi(x)$ using formulas (56) and (57). The computed normalized residues and poles of the function $G(s)$ as well as the computed sum $\sum A_n/|\rho_n|$ are summarized in Table 4. It is seen from Table 4 that the values of the computed normalized residues are between zero and one, and the calculated sum of the normalized residues is 0.9413156 for $q = 4$ and 0.9569588 for $q = 5$, respectively. The location of the recovered four poles for $q = 4$ and five poles for $q = 5$ lays in between $-10,000$ and -0.35 on the negative real semiaxis.

The recovered complex modulus and complex velocity of the continuous spectrum model were further used to estimate the quality factor Q and the phase velocity $c(\omega)$ over the frequency band between 10^{-2} and 10^2 Hz using formulas (19) and (21). Figure 4 represents the reconstruction of the quality factor Q (top) and the phase velocity (bottom) of the model versus frequency using the Padé approximants of two different orders. It is seen from the top part of Fig. 4 that the quality factor of the continuous spectrum model is almost nearly constant $Q \simeq 21$ and the recovered quality factors for $q = 4$ and $q = 5$ fit the frequency dependent Q values of the model very well in a range of frequency about $0.2 \sim 100$ Hz. The phase velocity increases with the frequency illustrated in the bottom part of Fig. 4. The true and reconstructed phase velocities also fit fairly well in the frequency band from 10^{-2} to 10^2 Hz.

We also calculated values of relative errors for the estimation of phase velocity, quality Q factor, complex velocity, and complex modulus at sample data points over the given frequency band demonstrated in Table 5.

Table 6 Reconstruction of relaxation times to yield a constant $Q = 100$ ($\omega = 2 \sim 50$ Hz) for data with noise 1.0%, 1.5% and 2.5% ($\tau_{\epsilon_n}^c$, $\tau_{\sigma_n}^c$ stand for the predicted values of relaxation times)

n	1	2	3	$\sum A_n/ \rho_n $	Noise
$\tau_{\epsilon_n}^c$ (s)	0.05282943	0.00750373	0.00169959	0.86628592	1.0%
$\tau_{\sigma_n}^c$ (s)	0.05278142	0.00750316	0.00169956		
$\tau_{\epsilon_n}^c$ (s)	0.04335840	0.00608435	0.00155169	0.84236140	1.5%
$\tau_{\sigma_n}^c$ (s)	0.04332566	0.00608397	0.00155166		
$\tau_{\epsilon_n}^c$ (s)	0.03318668	0.00380367	0.00093020	0.80980242	2.5%
$\tau_{\sigma_n}^c$ (s)	0.03316694	0.00380347	0.00093019		

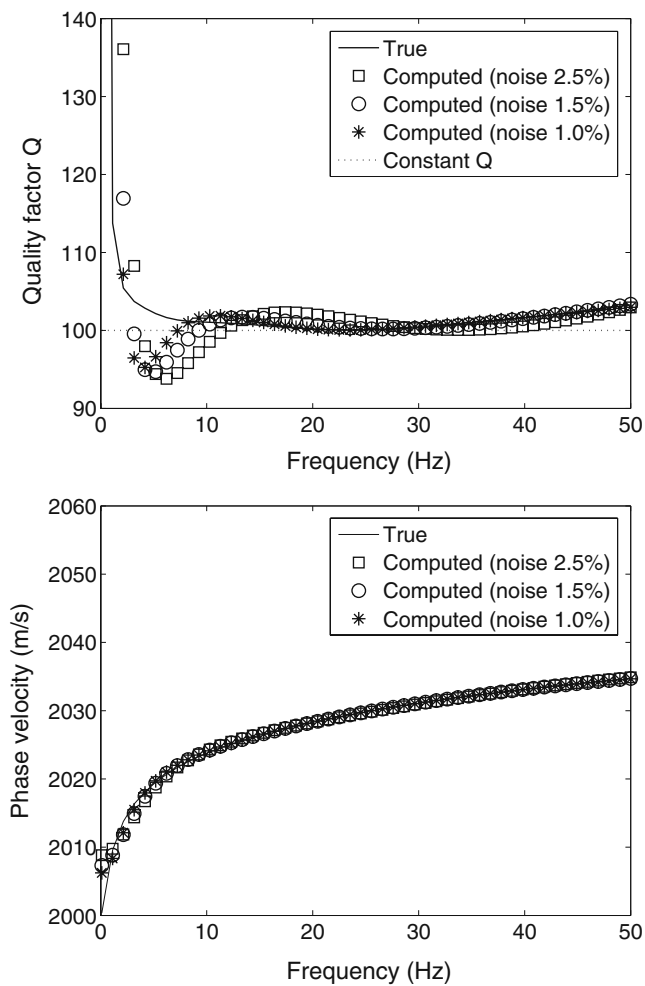


Fig. 5 True and computed quality factor Q (top) and phase velocity $c(\omega)$ (bottom) for data with 1.0%, 1.5% and 2.5% noise (SLS model)

In Table 5, the frequency band for calculation of relative errors of phase velocity, complex velocity, and complex modulus is from 0.01 to 100 Hz, and 0.2 ~ 100 Hz for the quality Q factors. The relative error formula follows

$$E_0 = \max_{1 \leq j \leq N} \left[\frac{|g(\omega_j) - \hat{g}(\omega_j)|}{|g(\omega_j)|} \right] \quad (55)$$

where ω_j ($j = 1, 2, \dots, N$) are the frequency sample data points and N is the total number of sample data. Here $g(\omega)$ represents the given frequency dependent function and $\hat{g}(\omega)$ the approximate function of $g(\omega)$, respectively.

6.3 Sensitivity analysis of the method

To numerically illustrate the sensitivity analysis of the estimated quality Q factors and phase velocities, a

uniformly distributed random noise was calculated as percentage of exact value at each measured data point for the SLS model as described in Section 6.1. We have performed numerical experiments to examine the sensitivity of the algorithm for different noise levels added to the input data. The same synthetic complex viscoelastic modulus is used as in Section 6.1. The order $q = p + 1 = 5$ in the inversion algorithm was chosen to reconstruct the strain-stress relaxation time parameters τ_{ϵ_n} and τ_{σ_n} using data with added noise. Table 6 shows the summary of the recovered values of τ_{ϵ_n} and τ_{σ_n} to yield a constant $Q = 100$ on the frequency band of 2 ~ 50 Hz together with the calculated values of $\sum A_n/|\rho_n|$ where $\sum A_n/|\rho_n| \approx 0.86628592$, $\sum A_n/|\rho_n| \approx 0.84236140$, and $\sum A_n/|\rho_n| \approx 0.80980242$ ($1 \leq n \leq 3$), corresponding to data with different noise levels 1.0%, 1.5%, and 2.5%, respectively.

In the numerical experiments any recovered pole ρ_n that is off the negative real semiaxis is discarded based on the inversion algorithm so that the total number of reconstructed relaxation mechanisms is less than $q = 5$ in each case of data with added noise. The reconstructed values of relaxation parameters τ_{ϵ_n} and τ_{σ_n} presented in Table 6 were used to evaluate the quality Q factors and phase velocities. Figure 5 illustrates the estimation of the quality Q factors (top) and phase velocities (bottom) for data with 1.0%, 1.5% and 2.5% noise corresponding to Table 6. The results of numerical computations show that even with added noise, the computed quality Q factors are nearly constant $Q = 100$ in the frequency band about $\omega = 10 \sim 40$ Hz, and the recovered phase velocities agree with the true values in the frequency range about $\omega = 2 \sim 50$ Hz. This demonstrates the stability of the reconstruction.

7 Conclusions

We developed a new numerical inversion method for estimation of quality Q factor and phase velocity in homogeneous dissipating media using Padé approximation. The approach is based on a rational ($[p, q]$ -Padé) approximation of the relaxation spectrum in the Stieltjes representation of the complex viscoelastic modulus. The problem is formulated as a constrained least squares minimization problem with regularization constraints provided by the Stieltjes representation of the complex modulus. Calculation of coefficients of Padé approximation is an ill-posed problem, and regularization is necessary to obtain an accurate solution. The method was tested using analytical models of viscoelastic media with a continuous spectrum as well as a standard linear solid

(Zener) model. The numerical results demonstrate the effectiveness of the developed approach. The method can be used for identification of relaxation parameters of viscoelastic materials from measurements of complex velocity or complex modulus. The recovered relaxation mechanisms can be used for simulation of seismic wavefields in viscoelastic media. Coefficients of low order Padé approximation provide coefficients of the differential equations for internal variables that allow efficiently reduce computation of viscoelastic problem to simulation of elastic wave equation. Our approach may provide significant savings in the computer memory and computation time needed for numerical simulation of seismic wave propagations in viscoelastic media.

Acknowledgements The authors would like to thank S.M. Day for providing valuable comments and discussions for the project, especially for the justification of the Proposition 1. We gratefully acknowledge generous support from NSERC, MITACS, PIMS, and sponsors of the POTSI and CREWES projects. The first author is also funded by a Postdoctoral Fellowship at the University of Calgary. The last author acknowledges partial support by NSF grants DMS-0508901 and DMS/CMG-0934721.

Appendix: Error estimate

Let function $\eta(x)$ satisfy the sum rule as in Proposition 1. In particular, $\eta(0) = \eta(0^+)$, our approximation method for the function $d\eta(x)$ implies that $\hat{\eta}(0) = \hat{\eta}(0^+)$. Let $d\xi(x)/dx$ and $d\hat{\xi}(x)/dx$ denote the normalized relaxation spectrum function and the approximate normalized relaxation spectrum function, respectively, such that for $x \in (0, \infty)$:

$$\xi(x) = \int_0^{x^+} \frac{d\eta(t)}{t}, \tag{56}$$

$$\hat{\xi}(x) = \int_0^{x^+} \frac{d\hat{\eta}(t)}{t} = \int_0^{x^+} \sum_{n=1}^q \frac{A_n}{|\rho_n|} \delta(t + \rho_n) dt \tag{57}$$

where A_n and ρ_n ($n = 1, 2, \dots, q$) are the poles and residues of the function $\hat{G}(s)$.

Proposition 2 *Function ξ is a non-decreasing function such that*

$$\lim_{x \rightarrow \infty} \xi(x) = 1. \tag{58}$$

Proof Noticing that ξ is the integral of a non-negative measure in (56), the verification of a non-decreasing

function ξ is given by the fact that $\xi(0) = 0$ and for $\forall x_1, x_2 \in [0, \infty), x_1 < x_2$,

$$\xi(x_2) - \xi(x_1) = \int_{x_1^+}^{x_2^+} \frac{d\eta(t)}{t} = \int_{x_1^+}^{x_2^+} \frac{\Phi(-\ln t) dt}{t} \geq 0. \tag{59}$$

The limit (58) is established by the sum rule property of the function η in Proposition 1. This completes the proof. \square

Theorem 1 *Assume that for given sufficiently small numbers $\epsilon_1 > 0, \epsilon_2 > 0$ and $\epsilon_3 > 0$ there exists a large enough number $T > |\rho_q| > 0$ such that*

$$\| \xi(x) - \hat{\xi}(x) \|_{L^2_{[0, T]}} < \epsilon_1, \tag{60}$$

$$1 - \epsilon_2 < \xi(T), \tag{61}$$

$$|1 - \hat{\xi}(x)| \leq \epsilon_3, \quad x \in [T, \infty). \tag{62}$$

The following error estimate of the q -th order rational approximation $\hat{G}(s)$ to the Stieltjes integral $G(s)$

$$|G(s) - \hat{G}(s)| \leq c_1 \epsilon_1 + c_2 \epsilon_2 + c_3 \epsilon_3 \tag{63}$$

holds for any $s = i\omega, \forall \omega \in [\omega_0, \infty)$, where

$$c_1 = \left[\frac{1}{2} \left(\frac{1}{T + \omega_0^2/T} \right) + \frac{\pi}{4\omega_0} \right]^{\frac{1}{2}}, \tag{64}$$

$$c_2 = \frac{\pi}{2} + \frac{2}{\sqrt{1 + \omega_0^2/T^2}}, \tag{65}$$

$$c_3 = \frac{1}{\sqrt{1 + \omega_0^2/T^2}}. \tag{66}$$

Proof By Proposition 2 and inequality (61), for the given sufficiently small number $\epsilon_2 > 0$, there exists a large enough number $T > |\rho_q| > 0$ such that

$$1 - \epsilon_2 < \xi(T) \leq \xi(x) < 1, \quad x \in [T, \infty). \tag{67}$$

For any $s = i\omega, \omega \in [\omega_0, \infty)$, we write

$$G(s) - \hat{G}(s) = \int_0^\infty \frac{d[\eta(x) - \hat{\eta}(x)]}{s + x} = I_1 + I_2 \tag{68}$$

where

$$I_1 = \int_0^{T^+} \frac{d[\eta(x) - \hat{\eta}(x)]}{s+x} = \int_0^{T^+} \frac{x}{s+x} d[\xi(x) - \hat{\xi}(x)], \tag{69}$$

$$I_2 = \int_{T^+}^{\infty} \frac{d[\eta(x) - \hat{\eta}(x)]}{s+x} = \int_{T^+}^{\infty} \frac{x}{s+x} d[\xi(x) - \hat{\xi}(x)]. \tag{70}$$

Next, we will estimate the above two integrals I_1 and I_2 . To estimate the integral I_1 , by the definition of ξ and $\hat{\xi}$ in (56–57), $\xi(0^+) = \hat{\xi}(0^+) = 0$, and using integration by parts on the right hand side of (69), we have

$$\begin{aligned} I_1 &= \frac{[\xi(x) - \hat{\xi}(x)]x}{s+x} \Big|_0^T - \int_0^{T^+} [\xi(x) - \hat{\xi}(x)] d\left(\frac{x}{s+x}\right) \\ &= \frac{[\xi(T) - \hat{\xi}(T)]T}{s+T} - \int_0^{T^+} [\xi(x) - \hat{\xi}(x)] \frac{s}{(s+x)^2} dx. \end{aligned}$$

We note that the second term on right hand side of the above equation can be estimated by the Cauchy–Schwarz inequality. Then, I_1 is estimated as

$$\begin{aligned} |I_1| &\leq \frac{|\xi(T) - \hat{\xi}(T)|T}{|s+T|} + \left[\int_0^{T^+} |\xi(x) - \hat{\xi}(x)|^2 dx \right]^{\frac{1}{2}} \\ &\quad \cdot \left[\int_0^{T^+} \left| \frac{s}{(s+x)^2} \right|^2 dx \right]^{\frac{1}{2}}. \end{aligned} \tag{71}$$

Since $\hat{\xi}(T) = \sum_{n=1}^q \frac{A_n}{|\rho_n|}$ and the inequalities (62) and (67) hold, we have

$$\left| 1 - \sum_{n=1}^q \frac{A_n}{|\rho_n|} \right| \leq \epsilon_3 \tag{72}$$

and

$$|\xi(T) - \hat{\xi}(T)| \leq |\xi(T) - 1| + \left| 1 - \sum_{n=1}^q \frac{A_n}{|\rho_n|} \right| \leq \epsilon_2 + \epsilon_3 \tag{73}$$

so that from (60) and (73), the estimate (71) becomes

$$\begin{aligned} |I_1| &\leq \frac{(\epsilon_2 + \epsilon_3)T}{|i\omega + T|} + \epsilon_1 \left[\int_0^{T^+} \frac{|i\omega|^2}{|i\omega + x|^4} dx \right]^{\frac{1}{2}} \\ &\leq \frac{(\epsilon_2 + \epsilon_3)T}{\sqrt{\omega^2 + T^2}} + \epsilon_1 \left[\int_0^{T^+} \frac{\omega^2}{(\omega^2 + x^2)^2} dx \right]^{\frac{1}{2}}. \end{aligned} \tag{74}$$

It should be noted that the definite integral under the square root term on the right hand side of (74) can be calculated as

$$\int_0^{T^+} \frac{\omega^2}{(\omega^2 + x^2)^2} dx = \frac{1}{2} \left(\frac{T}{T^2 + \omega^2} \right) + \frac{1}{2\omega} \arctan \left(\frac{T}{\omega} \right) \tag{75}$$

so that for $\omega \in [\omega_0, \infty)$,

$$\left| \int_0^{T^+} \frac{\omega^2}{(\omega^2 + x^2)^2} dx \right| \leq \frac{1}{2} \left(\frac{1}{T + \omega_0^2/T} \right) + \frac{\pi}{4\omega_0}. \tag{76}$$

Therefore, from (75) and (76), we obtain

$$|I_1| \leq c_1 \epsilon_1 + c_3 (\epsilon_2 + \epsilon_3) \tag{77}$$

where

$$c_1 = \left[\frac{1}{2} \left(\frac{1}{T + \omega_0^2/T} \right) + \frac{\pi}{4\omega_0} \right]^{\frac{1}{2}}, \quad c_3 = \left[1 + \frac{\omega_0^2}{T^2} \right]^{-\frac{1}{2}}. \tag{78}$$

To estimate I_2 , noticing (57), for $x > |\rho_q|$, we have

$$d\hat{\xi}(x) = \sum_{n=1}^q \frac{A_n}{|\rho_n|} \delta(x + \rho_n) = 0 \tag{79}$$

since $|\rho_q| = \max_{1 \leq n \leq q} |\rho_n|$. So the integral (70) can be rewritten as

$$I_2 = \int_{T^+}^{\infty} \frac{x}{s+x} d\xi(x) = \int_{T^+}^{\infty} \frac{x}{s+x} d[\xi(x) - 1]. \tag{80}$$

Then integration by parts gives

$$\begin{aligned} I_2 &= \frac{x}{s+x} [\xi(x) - 1] \Big|_{T^+}^{\infty} - \int_{T^+}^{\infty} [\xi(x) - 1] \frac{s}{(s+x)^2} dx \\ &= -\frac{[\xi(T) - 1]T}{s+T} - \int_{T^+}^{\infty} [\xi(x) - 1] \frac{s}{(s+x)^2} dx \end{aligned} \tag{81}$$

since $\lim_{x \rightarrow \infty} \xi(x) = 1$. Then, using (67), for $\omega \in [\omega_0, \infty)$, it follows from (81) that I_2 is estimated as

$$\begin{aligned} |I_2| &\leq \frac{|\xi(T) - 1|T}{|i\omega + T|} + \int_{T^+}^{\infty} |\xi(x) - 1| \frac{|i\omega|}{|i\omega + x|^2} dx \\ &\leq \frac{\epsilon_2 T}{\sqrt{\omega^2 + T^2}} + \epsilon_2 \int_{T^+}^{\infty} \frac{\omega}{\omega^2 + x^2} dx \\ &\leq \frac{\epsilon_2}{\sqrt{1 + \omega_0^2/T^2}} + \epsilon_2 \left[\frac{\pi}{2} - \arctan \left(\frac{T}{\omega} \right) \right]. \end{aligned} \tag{82}$$

Thus we get

$$|I_2| \leq \left(\frac{1}{\sqrt{1 + \omega_0^2/T^2}} + \frac{\pi}{2} \right) \epsilon_2. \quad (83)$$

For $\epsilon_1 > 0$, $\epsilon_2 > 0$, $\epsilon_3 > 0$ and $\omega \in [\omega_0, \infty)$, from (77) and (83), we obtain the following error estimate

$$|G(i\omega) - \hat{G}(i\omega)| \leq |I_1| + |I_2| \leq c_1\epsilon_1 + c_2\epsilon_2 + c_3\epsilon_3 \quad (84)$$

where c_1 , c_3 are given in (78), and

$$c_2 = \frac{\pi}{2} + \frac{2}{\sqrt{1 + \omega_0^2/T^2}}. \quad (85)$$

This completes the proof. \square

References

- Amundsen, L., Mittet, R.: Estimation of phase velocities and Q -factors from zero-offset, vertical seismic profile data. *Geophysics* **59**, 500–517 (1994)
- Baker Jr., G.A., Graves-Morris, P.: *Padé Approximations*. Cambridge University Press, Cambridge (1996)
- Bergman, D.J.: The dielectric constant of a composite material - a problem in classical physics. *Phys. Rep. C* **43**, 377–407 (1978)
- Bergman, D.J.: Exactly solvable microscopic geometries and rigorous bounds for the complex dielectric constant of a two-component composite material. *Phys. Rev. Lett.* **44**, 1285 (1980)
- Blanch, J.O., Robertsson, J.O.A., Symes, W.W.: Modeling of a constant Q : methodology and algorithm for an efficient and optimally inexpensive viscoelastic technique. *Geophysics* **60**, 176–184 (1995)
- Cheney, E.W.: *Introduction to Approximation Theory*, 2nd edn. Chelsea Publishing Company (1982)
- Carcione, J.M., Kosloff, D., Kosloff, R.: Wave propagation simulation in a linear viscoelastic medium. *Geophys. J. R. Astron. Soc.* **93**, 393–407 (1988)
- Carcione, J.M., Kosloff, D., Kosloff, R.: Wave propagation simulation in a linear viscoelastic medium. *Geophys. J. R. Astron. Soc.* **95**, 597–611 (1988)
- Carcione, J.M.: *Wave Fields in Real Media: wave propagation in anisotropic, anelastic, porous and electromagnetic media*, 2nd ed. Elsevier (2007)
- Cherkaev, E.: Inverse homogenization for evaluation of effective properties of a mixture. *Inverse Probl.* **17**, 1203–1218 (2001)
- Dasgupta, R., Clark, R.A.: Estimation of Q from surface seismic reflection data. *Geophysics* **63**, 2120–2128 (1998)
- Day, S.M., Minster, J.B.: Numerical simulation of attenuated wavefields using a Padé approximant method. *Geophys. J. R. Astron. Soc.* **78**, 105–118 (1984)
- Day, S.M.: Efficient simulation of constant Q using coarse-grained memory variables. *Bull. Seismol. Soc. Am.* **88**, 1051–1062 (1998)
- Day, S.M., Bradley, C.R.: Memory-efficient simulation of anelastic wave propagation. *Bull. Seismol. Soc. Am.* **91**, 520–531 (2001)
- Ely, G.P., Day, S.M., Minster, J.B.: A support-operator method for viscoelastic wave modelling in 3-D heterogeneous media. *Geophys. J. Int.* **172**, 331–344 (2008)
- Emmerich, E., Korn, M.: Incorporation of attenuation into time-domain computations of seismic wave fields. *Geophysics* **52**, 1252–1264 (1987)
- Emmerich, E.: *PSV-wave propagation in a medium with local heterogeneities: a hybrid formulation and its application*. *Geophys. J. Int.* **109**, 54–64 (1992)
- Fierro, R.D., Golub, G.H., Hansen, P.C., O’Leary, D.P.: Regularization by truncated total least squares. *SIAM J. Sci. Comput.* **18**, 1223–1241 (1997)
- Golden, K., Papanicolaou, G.: Bounds on effective parameters of heterogeneous media by analytic continuation. *Commun. Math. Phys.* **90**, 473–491 (1983)
- Golub, G.H., Hansen, P.C., O’Leary, D.P.: Tikhonov regularization and total least squares. *SIAM J. Matrix Anal. Appl.* **21**, 185–194 (1999)
- Graves, R.W., Day, S.M.: Stability and accuracy of coarse-grain viscoelastic simulations. *Bull. Seismol. Soc. Am.* **93**, 283–300 (2003)
- Kjartansson, E.: Constant Q -wave propagation and attenuation. *J. Geophys. Res.* **84**, 4737–4748 (1979)
- Kosloff, D., Baysal, E.: Forward modeling by a Fourier method. *Geophysics* **47**, 1402–1412 (1982)
- Krebes, E.S., Quiroaa-Goode, G.: A standard finite-difference scheme for the time-domain computation of anelastic wavefields. *Geophysics* **59**, 290–296 (1994)
- Liu, P., Achuleta, R.J.: Efficient modeling of Q for 3D numerical simulation of wave propagation. *Bull. Seismol. Soc. Am.* **96**, 1352–1358 (2006)
- Liu, H.P., Anderson, D.L., Kanamori, H.: Velocity dispersion due to anelasticity; implications for seismology and mantle composition. *Geophys. J. R. Astron. Soc.* **47**, 41–58 (1976)
- Margrave, G.F., Lamoureux, M.P., Grossman, J.P., Iliescu, V.: Gabor deconvolution of seismic data for source waveform and Q correction. In: 72nd Ann. Internat. Mtg., Soc. Expl. Geophys. pp. 714–717 (2002)
- Margrave, G.F., Gibson, P.C., Grossman, J.P., Henley, D.C., Iliescu, V., Lamoureux, M.P.: The Gabor transform, pseudodifferential operators, and seismic deconvolution. *Integr. Comput.-Aided Eng.* **12**, 43–55 (2005)
- Milton, G.W.: Bounds on the complex dielectric constant of a composite material. *Appl. Phys. Lett.* **37**, 300–302 (1980)
- Robertsson, J.O.A., Blanch, J.O., Symes, W.W.: Viscoelastic finite-difference modeling. *Geophysics* **59**, 1444–1456 (1994)
- Tal-Ezer, H., Carcione, J.M., Kosloff, D.: An accurate and efficient scheme for wave propagation in linear viscoelastic media. *Geophysics* **55**, 1366–1379 (1990)
- Tikhonov, A.N., Arsenin, V.Y.: *Solutions of Ill-posed Problems*. Wiley, New York (1977)
- Tonn, R.: The determination of the seismic quality factor Q from VSP data: a comparison of different computational methods. *Geophys. Prospect.* **39**, 1–27 (1991)
- Ursin, B., Toverud, T.: Comparison of seismic dispersion and attenuation models. *Stud. Geophys. Geod.* **46**, 293–320 (2002)
- Toverud, T., Ursin, B.: Comparison of seismic attenuation models using zero-offset vertical seismic profiling (VSP) data. *Geophysics* **70**, F17–F25 (2005)
- Wang, Y.: A stable and efficient approach of inverse Q filtering. *Geophysics* **67**, 657–663 (2002)
- Wang, Y.: Quantifying the effectiveness of stabilized inverse Q filtering. *Geophysics* **68**, 337–345 (2003)
- Widder, D.V.: *The Laplace Transform*. Princeton University Press, Princeton (1946)

39. Xu, T., McMechan, G.A.: Composite memory variables for viscoelastic synthetic seismograms. *Geophys. J. Int.* **121**, 634–639 (1995)
40. Zhang, C., Ulrych, T.J.: Estimation of quality factors from CMP records. *Geophysics* **67**, 1542–1547 (2002)
41. Zhang, C., Ulrych, T.J.: Seismic absorption compensation: A least squares inverse scheme. *Geophysics* **72**, R109–R114 (2007)
42. Zhang, D., Cherkaev, E.: Padé approximations for identification of air bubble volume from temperature or frequency dependent permittivity of a two-component mixture. *Inv. Prob. Sci. Eng.* **16**(4), 425–445 (2008)
43. Zhang, D., Cherkaev, E.: Reconstruction of spectral function from effective permittivity of a composite material using rational function approximations. *J. Comput. Phys.* **228**(15), 5390–5409 (2009)
44. Zhang, D., Lamoureux M.P., Margrave, G.F.: Estimation of Q and phase velocity using the stress-strain relaxation sepectrum. University of Calgary CREWES Research Report vol. 21 (2009)